

# The Effects of Mechanical Degradation and Viscoelastic Behavior on Injectivity of Polyacrylamide Solutions

R.S. Seright, SPE, Exxon Production Research Co.

## Abstract

Results of recent experiments that clarify the effects of mechanical degradation and viscoelastic behavior on the flow of partially hydrolyzed polyacrylamide solutions through porous media are presented. From these results, a simple model that may be used to predict injectivity of polyacrylamide solutions is developed.

Injection pressures for linear corefloods are shown to be separable into two components: (1) an initial pressure drop associated with the entrance of polymer into the sandstone and (2) a constant pressure gradient throughout the remainder of the core. Entrance pressure drop is zero until the polymer solution flux increases to the rate where mechanical degradation takes place. Thereafter, entrance pressure drop and the degree of polymer mechanical degradation increase with increasing flux. In addition, polymer solutions that undergo a large entrance pressure drop and a high degree of mechanical degradation when first injected into a core show no entrance pressure drop and no further degradation after reinjection into the same core at the same flux. These observations suggest that the entrance pressure drop is associated closely with the process of polymer mechanical degradation.

A new correlation is developed that may be used to determine entrance pressure drop and the level of mechanical degradation directly as a function of sandface flux, permeability, and porosity. This correlation is more convenient to apply and less dependent on flow geometry than previous correlations.

Based on these observations, a model is developed that may be used to estimate injectivity of polyacrylamide solutions in linear or radial flow geometries. This model takes into account the entrance pressure drop and the dilatant nature of the polymer near the wellbore. Predictions made with this model are compared with experimental results.

## Introduction

This paper reports an investigation of the influence of mechanical degradation and viscoelasticity on the injectivity of partially hydrolyzed polyacrylamide solutions. The viscoelastic nature of the polymer is important primarily at high fluxes that occur near a wellbore. However, mechanical degradation affects the mobility of a polymer bank at all positions within a reservoir. The approach in this report is first to re-examine the process of predicting polymer mechanical degradation in porous media and to simplify the prediction process so that it may more readily be applied to field situations. Next, results of recent experiments that clarify the effects of mechanical degradation and viscoelastic behavior on the flow of polyacrylamide solutions through porous media are presented. Finally, these results are used to develop a simple model to estimate injectivity impairment during a polymer flood.

## Mechanical Degradation

Mechanical degradation means that fluid stresses become large enough to fragment polymer molecules, resulting in an irreversible loss of viscosity and resistance factor. This may happen when a polymer solution is forced at high flux through a porous medium or through a constriction.

Resistance factor is defined as the ratio of brine mobility to the mobility of a polymer solution. It may be thought of as the apparent relative viscosity of a polymer solution in porous media. Resistance factors of polyacrylamide solutions are often greater than viscosities. This suggests that polyacrylamides reduce water mobility both by increasing solution viscosity and by reducing effective permeability to water.<sup>1,2</sup> Part of the permeability reduction is retained after a polyacrylamide bank is displaced by brine.

One method of assessing the degree of polymer mechanical degradation is to compare solution viscosities. However, another method is desired since

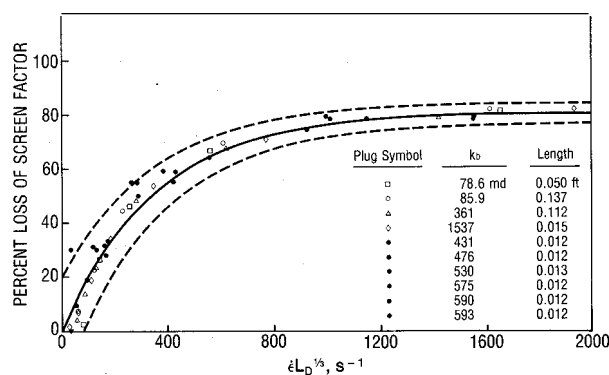


Fig. 1— $\epsilon L_D^{1/3}$  correlation, 600 ppm Polymer A in 3.3% brine forced through sandstone plugs; porosity=0.21; data furnished by Maerker (after Ref. 3).

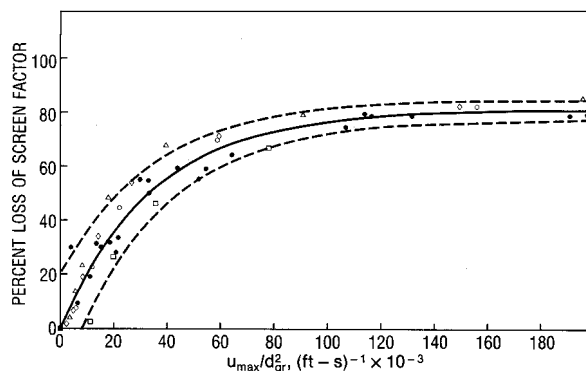


Fig. 2— $u_{\max}/d_{gr}^2$  correlation; same data as used in Fig. 1.

mechanical degradation often reduces resistance factor much more than it reduces viscosity.<sup>3</sup> Jennings *et al.*<sup>4</sup> suggested that screen-factor measurements more closely correlate with resistance factors. Screen factor is defined as the ratio of the time required for a fixed volume of polymer solution to flow through a stack of five 100-mesh screens to the flow time required for the same volume of brine to pass through the screens. Like resistance factors, screen factors often are larger and more sensitive to mechanical degradation than viscosities. Although screen factors may be measured conveniently and reproducibly, correlations between screen factors and resistance factors are empirical. Also, any screen-factor/resistance-factor correlation is valid only for solutions that have the same salinity, polymer concentration, polymer source, and temperature.<sup>4</sup>

Several attempts to predict the degree of polyacrylamide mechanical degradation in porous media have been reported.<sup>3,5-8</sup> Maerker<sup>3,6</sup> has conducted the most extensive investigation to date. He correlated percent loss of screen factor with the group  $\epsilon L_D^{1/3}$ , where

$$\epsilon = \text{stretch rate} = 2(\text{flux}) / (86,400 d_{gr} \phi),$$

seconds<sup>-1</sup>,

$$L_D = \text{dimensionless length} = (\text{actual core length}) / d_{gr},$$

$$d_{gr} = \text{average grain diameter}$$

$$= \frac{1-\phi}{\phi} \sqrt{\frac{150}{\phi} k_b 1.0623 \times 10^{-14}}, \text{ ft (m),}$$

$$k_b = \text{permeability to brine, md,}$$

and

$$\phi = \text{porosity.}$$

Fig. 1 shows Maerker's data. The solid curve represents a non-linear least-squares fit to a two-parameter exponential decay model. The dashed curves represent limits associated with  $\pm 10\%$  experimental

uncertainty in the determination of screen factors and permeabilities. Maerker's correlation worked well for consolidated sandstone plugs with permeabilities ranging from 78 to 1,537 md. Another factor,  $\phi^m$ , was introduced to account for degradation in unconsolidated sands. The exponent  $m$  is an empirical quantity that depends on the screen factor. This requires an iterative procedure to predict mechanical degradation.

Morris and Jackson<sup>7</sup> correlated percent loss of screen factor with the group,  $\epsilon L_D^{(M/10^7)}$ , where  $M$  is the polymer molecular weight. Although this correlation suggests that core length has a very important influence on the degree of mechanical degradation, experimental verification was not reported.

The presence of a length dependence complicates the prediction of polymer mechanical degradation in nonlinear geometries. With the correlations of Maerker and of Morris and Jackson, complex procedures must be used to predict degradation for typical wellbore geometries—e.g., radial (openhole, perforated), hemispherical (collapsed perforations), or some other (such as fractures).

An alternative correlation that considerably simplifies the process of predicting degradation is introduced here. Screen factor is correlated with the group  $u_{\max}/d_{gr}^2$ , where  $u_{\max}$  is the maximum polymer solution flux at the sandface. Figs. 1 and 2 provide a comparison of Maerker's  $\epsilon L_D^{1/3}$  correlation and the  $u_{\max}/d_{gr}^2$  correlation for consolidated sandstone plugs. Although Maerker's correlation appears to give a slightly better fit, both correlations fall within experimental error. The scatter in both cases may be attributed to the 5 to 10% experimental error that is typically associated with the determination of screen factors and permeabilities.

In Fig. 3, screen factor is correlated rather than percent loss of screen factor. The  $u_{\max}/d_{gr}^2$  correlation works well for consolidated and unconsolidated sands and for radial and linear cores with permeabilities ranging from 78 to 57,600 md, porosities ranging from 0.20 to 0.32, and lengths ranging from 0.01 to 1.0 ft (0.003 to 0.3 m). This correlation avoids the iterative procedure associated with Maerker's  $\phi^m$  term. Also, since the  $u_{\max}/d_{gr}^2$  correlation involves no length dependence, it

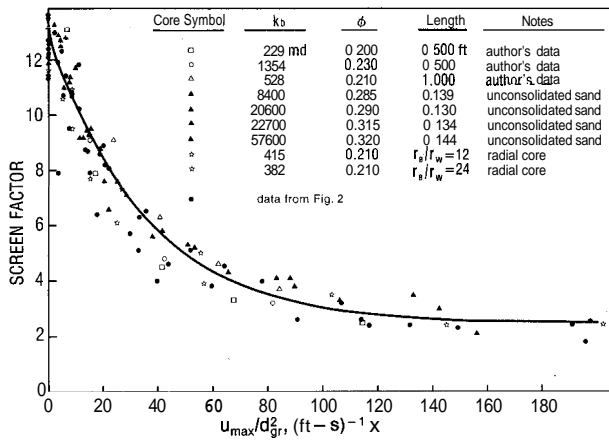


Fig. 3—Screen factor vs.  $u_{\max}/d_{gr}^2$ ; data furnished by Maerker (after Ref. 3) except as noted.

may be applied directly to any geometry. The solid curve in Fig. 3 represents a nonlinear least-squares fit of the data to a three-parameter exponential decay model.

Successful correlation of results from both radial and linear cores of various dimensions justifies the neglect of a length dependence. The intent here is not to deny that the process of mechanical degradation occurs over a finite distance. Instead, it is suggested that the interval required for the largest fraction of degradation to take place is negligible for purposes considered here. This approximation substantially simplifies prediction of polyacrylamide mechanical degradation in porous media.

### Factors Affecting Injectivity of Polyacrylamide Solutions

Injectivity during a polymer flood is influenced by several factors in addition to those affecting a water-flood. There are several ways in which polyacrylamides can form gels that may plug an injection well. First, gels may form if the polymer is not dispersed properly before injection. Second, gels may form when completely dissolved polymers are crosslinked by multivalent ions present in the injection water or in the reservoir brine. Polyacrylamides may also form gels by flocculating suspended particulate matter or by reacting with minerals in a formation.

The rheology of polymer solutions also has an important effect on injectivity. Viscometric studies show that polyacrylamide solutions are pseudoplastic.<sup>9</sup> On the basis of this information alone, one would expect resistance factor (apparent polymer solution relative viscosity) to decrease with increased polymer flux; however, polyacrylamide solutions actually exhibit an apparent dilatant behavior when flowing through porous media.<sup>1,2,4</sup> This apparent anomaly is attributed to the viscoelastic character of the polymer. One may rationalize that at low flux the characteristic relaxation time of the polymer solution is short relative to the characteristic time for deformation, and the solution has adequate time to respond to the tortuous flow path through the porous medium. In this case, the solution's viscous nature dominates. However, at high flux the characteristic time for deformation in flow through small

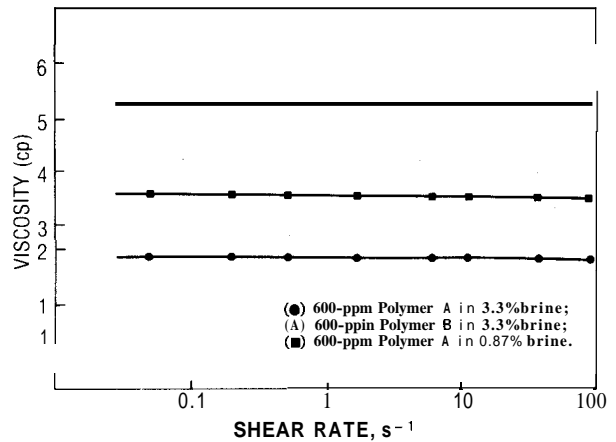


Fig. 4—Viscosity vs. shear rate.

constrictions may be of the same magnitude as the polymer relaxation time. In this situation, the elastic character creates a dramatically increased resistance to flow. One might expect the polymer's pseudoplastic nature to compete with its viscoelastic nature in porous media. Indeed, this competition has been observed for polyacrylamide solutions with low salinities.<sup>10</sup> However, for dilute polyacrylamide solutions with moderate to high salinities, the polymer's pseudoplastic behavior is minimized.<sup>9</sup> Fig. 4 illustrates this point for solutions of 600 ppm polyacrylamide in 3.3% brine and in 0.87% brine. Viscosity changes by less than 10% as shear rate increases from 0.06 to 100 seconds<sup>-1</sup>. These data were obtained with a Contraves Low Shear 30<sup>TM</sup> viscometer.

Near a wellbore, where flux is high, both mechanical degradation and viscoelasticity have large roles in determining polyacrylamide injectivity. To quantify these effects, polymer solutions were forced through 6-in.- (15-cm-) long sandstone cores at various flow rates. The polymer solutions consisted of 600 ppm polyacrylamide in 3.3% brine [3% NaCl, 0.3% CaCl<sub>2</sub>, pH=7, 25°C (77°F)]. Two commercially available polyacrylamides were used. Polymer A is supplied as a dry powder. Polymer B is supplied as a gel material consisting of about 25% polymer and 75% water. Both polymers are composed of about 30% acrylate groups and 70% acrylamide groups. For each injection rate, five pressure readings were obtained. One pressure tap was located just before the core inlet; three taps were located along the length of the core; and the fifth reading, atmospheric pressure, was associated with the core outlet (100% core length).

After determination of porosity and permeability to brine, 10 PV of polymer were forced through the core at a high flux. This solution was discarded. Then, pressures and flow rates were recorded while the next 5 to 10 fluid PV were collected. Then the flux was reduced, the first 2 to 5 PV were discarded, and the next 5 to 10 PV were collected while pressures and flow rates were recorded. This process was repeated until a low flux was attained. Pressures and flow rates stabilized quickly, and polymer solutions experienced no concentration loss as a result of passing through a core. Experimental results are listed in Tables 1 through 6.

TABLE 1—LINEAR COREFLOOD RESULTS FOR 600 ppm POLYMER A IN 3.3% BRINE  
(229-md Berea core, 6-in. length,  $\phi = 0.20$ )

$P_{0\%}$	Pressure* (psi)				Correlation Coefficient	Flux (ft/D)	$F_r$	$\Delta p_{md}$ (psi)	Screen Factor	Viscosity (cp)
	$P_{19\%}$	$P_{57\%}$	$P_{84\%}$	$P_{intercept}$						
0.53	—	—	—	0.53	—	0	—	—	17.8	2.44
8	6.6	3.7	1.8	8	0.998	0.38	4.9	0	17.8	2.44
20	16.2	8.6	3.3	20	1.000	3.7	6.4	0	17.0	2.43
40	31.7	16.5	5.9	39	1.000	10.7	10.6	1	16.1	2.41
75	57.9	28.8	9.5	71	0.000	17.7	11.6	4	13.1	2.39
177	123	59	15.5	150	0.996	43.6	10.0	27	7.9	2.13
313	207	98	23	252	0.995	105	6.9	61	4.5	1.88
432	283	133	—	343	0.998	171	5.8	89	3.3	1.70
586	382	183	—	464	0.998	289	4.6	122	2.5	1.67

\* $P_{x\%}$  = pressure at  $x\%$  core length (Fig. 5).  $P_{100\%} = 0$  psig.  $P_{intercept}$  and correlation coefficients were determined by linear regression, using all points except  $x = 0$ .

TABLE 2—LINEAR COREFLOOD RESULTS FOR 600 ppm POLYMER A IN 3.3% BRINE  
(1,354-md Bartlesville core, 6-in. length,  $\phi = 0.237$ )

$P_{0\%}$	Pressure (psi)				Correlation Coefficient	Flux (ft/D)	$F_r$	$\Delta p_{md}$ (psi)	Screen Factor	Viscosity (cp)
	$P_{18\%}$	$P_{55\%}$	$P_{88\%}$	$P_{intercept}$						
1.2	—	—	—	1.2	—	0	—	—	18.9	2.43
7.8	6.4	3.5	1.0	7.8	1.000	5.5	3.8	0	18.7	2.41
15	12.3	6.8	1.9	15	1.000	16.1	8.3	0	18.0	2.40
30	23.7	13.3	3.9	29	1.000	23.0	11.2	0	17.4	2.37
70	53.3	29.2	8.8	65	1.000	34.0	14.6	1	16.6	2.33
153	106	58	16.5	129	1.000	62.3	17.8	5	13.7	2.24
300	200	107	32	242	1.000	138	15.9	24	9.1	2.13
443	290	158	43	353	1.000	385	10.8	58	4.8	1.79
						743	8.1	90	3.2	1.73

TABLE 3—LINEAR COREFLOOD RESULTS FOR 600 ppm POLYMER A IN 3.3% BRINE  
(150-md Berea core, 6-in. length,  $\phi = 0.215$ )

$P_{0\%}$	Pressure (psi)				Correlation Coefficient	Flux (ft/D)	$F_r$	$\Delta p_{md}$ (psi)	Screen Factor	Viscosity (cp)
	$P_{19\%}$	$P_{49\%}$	$P_{81\%}$	$P_{intercept}$						
253	178	107	29	218	0.997	0	—	—	18.1	2.56
7	5.9	3.8	1.5	7	1.000	42.1	9.6	35	6.5	2.10
20	16.2	10.3	3.8	20	1.000	7.1	1.8	0	6.2	2.14
55	44	30	10.0	55	0.998	15.3	2.4	0	6.2	2.14
110	88	59	18.7	110	0.998	25.5	4.0	0	6.1	2.11
157	126	83	26	157	0.999	34.1	6.0	0	6.0	2.08
204	164	105	31	204	0.999	41.6	7.0	0	5.6	2.05
248	193	121	34	239	0.999	49.2	7.7	0	5.2	2.08
						56.4	7.9	9	4.8	2.02

\*Data directly above the asterisks concern a freshly prepared polymer solution that was forced once through a core at high flux. This solution was then reinjected into the same core to obtain the listings below the asterisks.

Screen factors, viscosities, and polymer concentration of the effluent were recorded and compared with those of the injected polymer solution. Screen factors were measured with a Dow screen viscometer; viscosities were measured at a shear rate of 11 seconds<sup>-1</sup> with a Contraves Low Shear 30 viscometer; and polymer concentrations were determined with a Waters Assocs. liquid chromatograph.

Injection of brine usually resulted in a constant pressure gradient throughout a core (Fig. 5). This indicates that the cores were reasonably homogeneous. Injection of polymer at low flux—so that no polymer mechanical degradation was detected—also resulted in a constant pressure gradient throughout the core. This meant that resistance factor was also constant throughout the core. When polymer was injected at high flux, a con-

stant pressure gradient was observed throughout the core except across the inlet sandface. The pressure drop between the first two pressure taps was greater than expected. A linear regression may be performed by using the last four of the five pressure readings and their respective positions. Correlation coefficients were usually greater than 0.99, indicating that polymer mobility was remarkably independent of core length. The pressure intercept from this regression estimates the pressure just inside the inlet sandface. The difference between the observed injection pressure and this pressure intercept is defined as the “entrance pressure drop,”  $\Delta p_{md}$ .

A resistance factor,  $F_r$ , is obtained for each polymer flux by dividing the brine mobility,  $\lambda_b$ , by the polymer mobility  $A_p$ . Thus, for each polymer flux an entrance

**TABLE 4—LINEAR COREFLOOD RESULTS FOR 600 ppm POLYMER B IN 3.3% BRINE  
(232-md Berea core, 6-in. length,  $\phi = 0.199$ )**

Pressure (psi)					Correlation Coefficient	Flux (ft/D)	$F_r$	$\Delta p_{md}$ (psi)	Screen Factor	Viscosity (cp)
$p_{0\%}$	$p_{28\%}$	$p_{58\%}$	$p_{84\%}$	$p_{intercept}$						
						0	—	—	33.6	5.03
5.4	4.0	1.8	0.7	5.4	0.999	0.67	26.5	0	30.7	4.91
34	24	13.9	5.7	34	1.000	3.1	31.5	0	30.1	4.56
75	54	31	13.3	75	1.000	5.3	42.2	0	29.0	4.44
181	125	73	27.5	175	1.000	10.5	48.8	6	21.1	4.08
315	200	113	43	278	1.000	23.1	35.3	37	12.0	3.02
467	278	158	60	387	1.000	50.3	22.6	80	7.2	2.90
590	342	196	75	477	1.000	85.4	16.4	113	5.1	2.49

**TABLE 5—LINEAR COREFLOOD RESULTS FOR 600 ppm POLYMER B IN 3.3% BRINE  
(1,895-md Bartlesville core, 6-in. length,  $\phi = 0.237$ )**

Pressure (psi)					Correlation Coefficient	Flux (ft/D)	$F_r$	$\Delta p_{md}$ (psi)	Screen Factor	Viscosity (cp)
$P_{0\%}$	$P_{20\%}$	$P_{60\%}$	$P_{88\%}$	$P_{intercept}$						
						0	—	—	35.6	5.60
5.9	4.6	2.1	0.7	5.9	0.999	8.9	18.4	0	35.5	5.60
18.0	14.4	7.3	2.1	18	1.000	14.5	33.7	0	35.4	5.56
35	28.1	14.7	4.4	35	1.000	20.1	48.0	0	34.8	5.45
70	55.7	28.9	8.7	70	1.000	29.7	64.0	0	31.7	5.36
165	118	58	16	147	1.000	62.8	63.9	18	21.7	4.83
313	207	102	28	258	1.000	193	36.5	55	9.9	3.45
455	295	146	43	368	1.000	429	23.4	87	5.5	2.76
596	387	193	46	483	1.000	758	17.4	113	3.8	2.41

**TABLE 6—LINEAR COREFLOOD RESULTS FOR 600 ppm POLYMER B IN 3.3% BRINE  
(1,223-md Bartlesville core, 6-in. length,  $\phi = 0.237$ )**

Pressure (psi)					Correlation Coefficient	Flux (ft/D)	$F_r$	$\Delta p_{md}$ (psi)	Screen Factor	Viscosity (cp)
$p_{0\%}$	$p_{19\%}$	$p_{57\%}$	$p_{84\%}$	$p_{intercept}$						
						0	—	—	37.2	5.30
440	272	154	59	366	0.999	166	27.8	74	7.8	3.18
0.5	0.35			0.5	1.000	2.8	2.6	0	7.6	3.08
1.3	0.93	—	—	1.3	1.000	6.0	3.3	0	7.6	3.08
8.0	5.8	3.5	1.4	8.0	1.000	29.4	4.2	0	7.5	3.07
16.0	11.7	7.0	2.9	16.0	1.000	52.6	4.7	0	7.4	3.07
35	25.8	15.4	6.5	35	1.000	87.7	6.2	0	7.5	3.07
75	57	34	13.5	75	1.000	123.3	9.6	0	7.5	3.07
150	112	68	28	150	1.000	163.3	14.3	0	7.3	3.05
292	217	139	52	292	0.999	231.6	19.6	0	6.5	2.95
433	307	179	71	415	1.000	323	27.8	18	5.5	2.70

\*Data directly above the asterisks concern a freshly prepared polymer solution that was forced once through a core at high flux. This solution was then reinjected into the same core to obtain the listings below the asterisks.

pressure drop,  $\Delta p_{md}$ , and a resistance factor,  $F_r$ , are obtained. Tables 1 through 6 list the results of experiments with both high- and low-permeability cores.

Figs. 6 and 7 provide evidence suggesting that the entrance pressure drop is associated with polymer mechanical degradation. First, the entrance pressure drop correlates well using the same  $u_{max}/d_{gr}^2$  group that was used to correlate levels of mechanical degradation (screen factors). Second, when polymer solutions are injected at low flux, so that the polymer undergoes no significant loss of screen factor or viscosity, the entrance pressure drop is zero. An entrance pressure drop is not observed until some polymer mechanical degradation is detected. Also, the greater the entrance pressure drop, the more degradation the polymer sustains.

Tables 3 and 6 provide further evidence that the entrance pressure drop is associated with mechanical degradation. These tables list results of experiments in which polyacrylamide solutions were first forced through sandstone cores at a high flux and then reinjected into the same cores at a variety of fluxes. A significant entrance pressure drop and a significant amount of degradation were found when freshly prepared polyacrylamide solutions were forced through the cores at high flux. However, when these solutions were reinjected into the same cores, no entrance pressure drop and no further significant degradation were observed at all fluxes up to that at which the solution was first injected. Furthermore, an entrance pressure drop and additional degradation were not detected until the

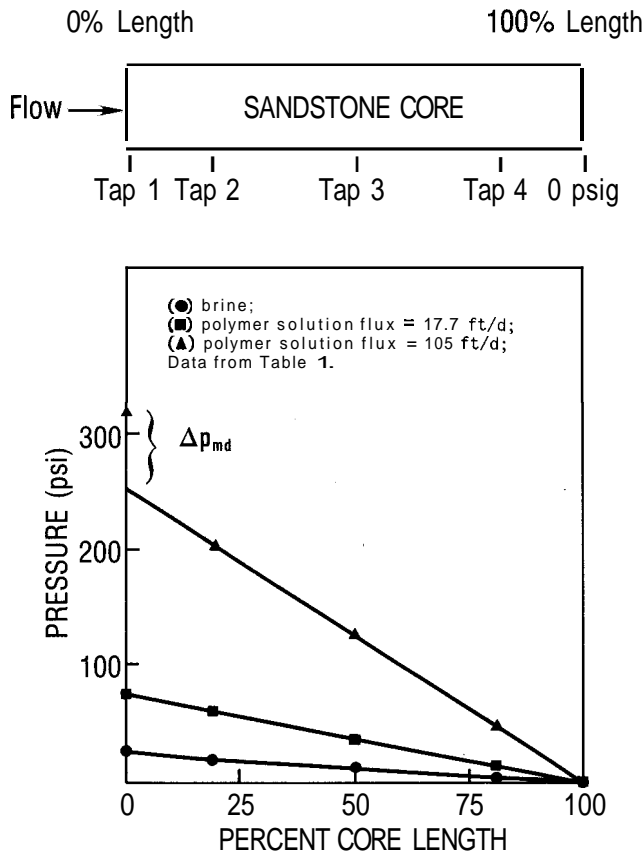


Fig. 5—Pressure vs. percent core length.

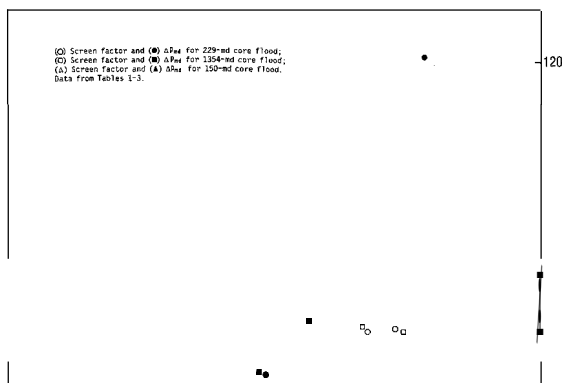


Fig. 6—Screen factor and entrance pressure drop vs.  $u_{\max}/d_{gr}^2$  (600 ppm Polymer B in 3.3% brine).

solution was reinjected at a flux exceeding the original injection flux.

These observations suggest a significant simplification of the process of predicting injectivity of polyacrylamide solutions. First, they allow the use of the  $u_{\max}/d_{gr}^2$  correlation when estimating the degree of polymer mechanical degradation and the entrance pressure drop. Second, they suggest that mechanical degradation effects are, for practical purposes, confined to the sandface. (This assumes that the injected polymer solution will never encounter a  $u_{\max}/d_{gr}^2$  value higher than that experienced at the sandface.)

Because of the radial flow geometry surrounding an injection well, fluid flux will vary inversely with distance from the wellbore. Thus, as a non-Newtonian fluid penetrates deeper into a formation, the resistance factor will vary. Figs. 8 and 9 illustrate how resistance factor varies with flux for polyacrylamide solutions that have sustained a fixed level of mechanical degradation. The apparent dilatant or viscoelastic nature of polyacrylamide solutions in porous media is evident at the higher fluxes. Resistance factor increases with flux to a maximum,  $(F_r)_{\max}$ . Exceeding the flux,  $u_{\max}$ , associated with this maximum resistance factor will result in additional degradation.

A polyacrylamide solution will exhibit its maximum resistance factor,  $(F_r)_{\max}$ , immediately inside the sandface. Then, because of the radial geometry, the flux and the resistance factor will decrease as the polymer solution penetrates deeper into the formation. After the polymer solution has penetrated three or four wellbore radii into the formation (that is, after the flux has decreased by a factor of three or four), the resistance factor appears to become flux independent. This further simplifies the model. The viscoelastic, flux-dependent behavior of polyacrylamide solutions can be confined to the near-wellbore region, while resistance factor can be assumed to be flux independent—possessing a value  $(F_r)_{\min}$ —elsewhere.

The assumption of flux-independent resistance factors when flux is very low is justified because viscometric data (Fig. 4 and Ref. 9) show that the solutions considered here (low polymer concentrations and moderate to high salinities) behave in a Newtonian fashion—especially at low shear rates. Thus, a change of resistance-factor behavior at ultralow flux is unlikely.

The task remains to quantify the rheology of polyacrylamide solutions that have had a fixed level of mechanical degradation at the sandface. A simple, functional relation between resistance factor and flux is desired. Figs. 8 and 9 illustrate typical resistance factor,  $F_r$ , vs. flux,  $u$ , data that the desired function should describe. A function of the type

$$F_r = (F_r)_{\min} + [(F_r)_{\max} - (F_r)_{\min}](u/u_{\max})^n \quad \dots (1)$$

is suggested, where  $u_{\max}$  is the maximum flux experienced by the polymer solution. Regression on the data in Figs. 8 and 9 and in Tables 1 through 6 reveals that the exponent  $n \approx 3$ .

For a given injection flux,  $(F_r)_{\max}$  (and  $\Delta p_{md}$ ) can be obtained directly by injecting a fresh polymer solution into a linear core and by measuring the resistance factor. Then,  $(F_r)_{\min}$  is obtained by reinjecting this solution in-

to the core at a low flux.  $(F_r)_{\min}$  may be approximated by using an alternative approach.  $(F_r)_{\min}$  will be largest  $[(F_r)_{\min 1}]$  if the polymer has undergone no mechanical degradation.  $(F_r)_{\min}$  will be smallest—approximately equal to the solution viscosity—after severe mechanical degradation. One may assume that  $(F_r)_{\min}$  increases linearly with screen factor between these two extremes. Let  $F_{s1}$  be the screen factor for the case of no degradation and  $F_{s2}$  be the screen factor for severe degradation. Then.

$$(F_r)_{\min} = \mu + [(F_r)_{\min 1} - \mu] \frac{F_s - F_{s2}}{F_{s1} - F_{s2}} \dots \dots \dots (2)$$

Where time permits, experiments can and should be performed to determine  $n$ ,  $(F_r)_{\min}$ , and  $\Delta p_{md}$  accurately for a given brine/polymer system.

### Injectivity Model

Injectivity is defined as the injection rate (injected volume per unit of time) divided by the injection pressure drop:

$$I_p = q/\Delta p \dots \dots \dots (3)$$

When injectivity of polyacrylamide solutions is predicted, the injection pressure drop may be separated into several components, including the following.

$\Delta p_{md}$  is the entrance pressure drop associated with polymer mechanical degradation at the sandface.

$\Delta p_v$  is the pressure drop associated with dilatant or viscoelastic polymer behavior near a wellbore.

$A_p$  is the pressure drop associated with polymer solutions flowing at low fluxes and exhibiting a Newtonian or flux-independent behavior.

$\Delta p_{ob}$  is the pressure drop associated with the flow of brine and oil.

The injection pressure drop,  $A_p$ , is simply the sum of these contributions.

### Application of the Injectivity Model to a Radial Coreflood

The injectivity model will be used now to estimate injectivities of polyacrylamide solutions during radial floods. These predictions will be compared with experimental results obtained from steady-state polymer floods involving pie-shape rocks. In a flood of this type, the injection pressure drop is given by

$$\Delta p = \Delta p_{md} + \Delta p_v + \Delta p_n \dots \dots \dots (4)$$

Since no brine or oil is flowing during these floods,  $\Delta p_{ob}$  is zero. If the permeability, porosity, and sandface area are known, the entrance pressure drop,  $\Delta p_{md}$ , may be estimated for any injection rate by using the  $u_{\max}/d_{gr}^2$  correlation (Figs. 6 and 7). To estimate  $A_p$ , and  $\Delta p_n$ , linear coreflood data like those plotted in Figs. 10 and 11 must be adapted for use in a radial geometry. In Figs. 10 and 11,  $(F_r)_{\max}$  was determined from data in Tables 1 and 4, respectively.  $(F_r)_{\min}$  was determined from Eq. 2 and Tables 1 and 4. During radial flow, flux is inversely proportional to radius, so Eq. 1 becomes

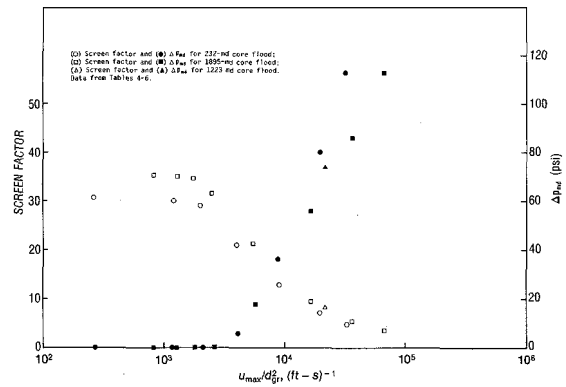


Fig. 7—Screen factor and entrance pressure drop vs.  $u_{\max}/d_{gr}^2$  (600 ppm Polymer B in 3.3% brine).

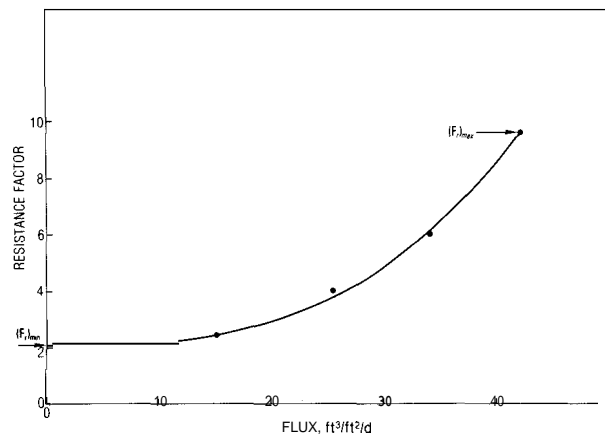


Fig. 8—Resistance factor vs. flux at constant screen factor (600 ppm Polymer A in 3.3% brine; data from Table 3; solid curve calculated from Eq. 1; assumes  $(F_r)_{\min} = 2.1$ ,  $(F_r)_{\max} = 9.6$ ,  $u_{\max} = 42.1$  ft/D, and  $n = 3$ ).

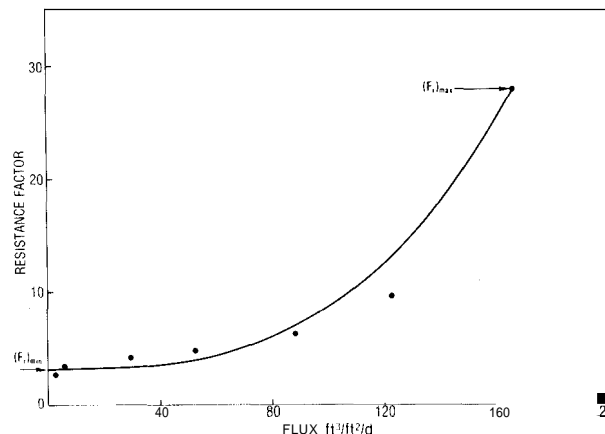


Fig. 9—Resistance factor vs. flux at constant screen factor (600 ppm Polymer B in 3.3% brine; data from Table 6; solid curve calculated from Eq. 1; assumes  $(F_r)_{\min} = 3.1$ ,  $(F_r)_{\max} = 27.8$ ,  $u_{\max} = 166$  ft/D, and  $n = 3$ ).

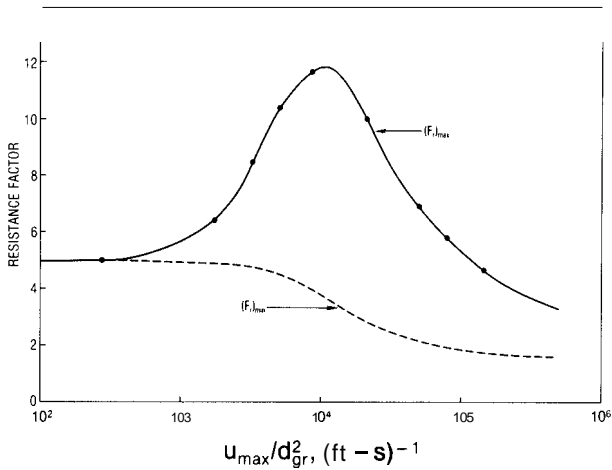


Fig. 10—Resistance factor vs.  $u_{\max}/d_{gr}^2$  (600 ppm Polymer A in 3.3% brine; data from Table 1).

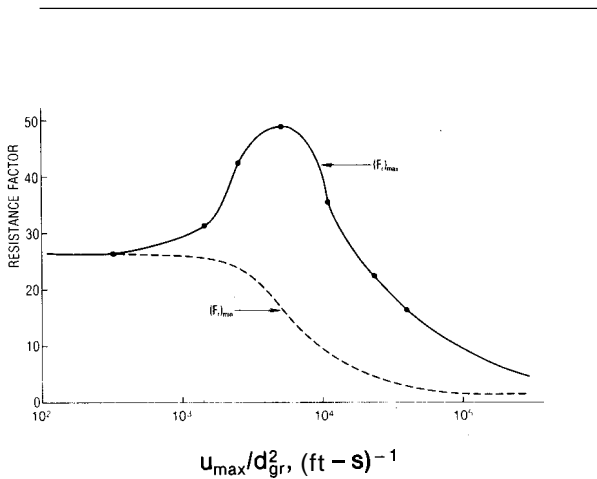


Fig. 11—Resistance factor vs.  $u_{\max}/d_{gr}^2$  (600 ppm Polymer B in 3.3% brine; data from Table 4).

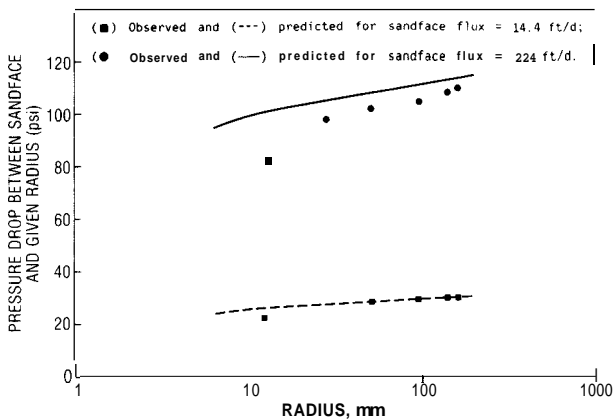


Fig. 12—Radial coreflood results (600 ppm Polymer A in 3.3% brine; data from Table 7).

$$F_r = (F_r)_{\min} + [(F_r)_{\max} - (F_r)_{\min}] \left( \frac{r_w}{r} \right)^n \dots (5)$$

Applying the Darcy equation to radial flow gives

$$q = -\phi r h \lambda_p \frac{dp}{dr} \dots (6)$$

and using the definition of resistance factor,

$$F_r = \frac{\Delta p}{q}, \dots (7)$$

along with Eq. 5 gives

$$dp = \frac{-q}{\theta r h \lambda_b} \left\{ (F_r)_{\min} + [(F_r)_{\max} - (F_r)_{\min}] \left( \frac{r_w}{r} \right)^n \right\} dr \dots (8)$$

Integrating between the sandface radius,  $r_w$ , and the radius of interest,  $r$ , yields

$$-\Delta p = \frac{-q}{\theta h \lambda_b} (F_r)_{\min} \ln \frac{r}{r_w} + \frac{q}{\theta h n \lambda_b} [(F_r)_{\max} - (F_r)_{\min}] \left[ 1 - \left( \frac{r_w}{r} \right)^n \right] \dots (9)$$

Here we define  $\Delta p_r$  and  $\Delta p_v$  as

$$\Delta p_r = \frac{q}{\theta h \lambda_b} (F_r)_{\min} \ln \left( \frac{r}{r_w} \right), \dots (10)$$

and

$$\Delta p_v = \frac{q}{\theta h n \lambda_b} [(F_r)_{\max} - (F_r)_{\min}] \left[ 1 - \left( \frac{r_w}{r} \right)^n \right] \dots (11)$$

To test the injectivity model, solutions consisting of 600 ppm polyacrylamide in 3.3% brine were forced through pie-shape ( $\theta = \pi/4$ ) cores at several flow rates. For each injection rate, pressure readings were recorded at several locations throughout the core. Tables 7 and 8 list the experimental results. These results were then compared with predictions based on Eqs. 3, 4, 10, and 11. Figs. 6, 7, 10, and 11 were used to obtain  $\Delta p_{md}$ ,  $(F_r)_{\max}$ , and  $(F_r)_{\min}$  values. Figs. 12 and 13 show predicted and observed pressure drops between the sandface and various distances. The predictions match the observed results reasonably well at both high and low injection

**TABLE 7—RADIAL (PIE-SHAPE) COREFLOOD RESULTS FOR 600 ppm POLYMER A IN 3.3% BRINE**  
 (375-md Berea core,  $\phi = 0.21$ , sandface area = 64 mm<sup>2</sup>, inner radius = 6.4 mm, external radius = 162 mm, height = 12.7 mm, sector angle =  $\pi/4$ )

Sandface Flux (ft/D)	Pressure* (psi)						Screen Factor	Viscosity (cp)
	$p_{6.4}$	$p_{12.7}$	$p_{28.6}$	$p_{50.8}$	$p_{95.3}$	$p_{139.7}$		
0	—	—	—	—	—	—	17.5	2.53
15.7	7	1.7	—	0.7	—	—	15.2	2.45
32.3	15	3.5	—	1.1	—	—	12.3	2.38
64.8	30	7.0	—	2.1	0.9	0.3	8.8	2.22
143	60	14	—	4.0	1.8	0.5	5.8	2.01
331	110	28	12	8.0	4.7	1.2	3.6	1.83
609	160	46	21	13	7.0	1.7	2.6	1.72
989	222	67	34	21	9.3	2.4	2.0	1.57
1,436	292	94	50	30	9.7	3.3	1.8	1.53

\*Pressure at radius  $r$

**TABLE 8—RADIAL (PIE-SHAPE) COREFLOOD RESULTS FOR 600 ppm POLYMER A IN 3.3% BRINE**  
 (375-md Berea core,  $\phi = 0.21$ , sandface area = 64 mm<sup>2</sup>, inner radius = 6.4 mm, external radius = 162 mm, height = 12.7 mm, sector angle =  $\pi/4$ )

Sandface Flux (ft/D)	Pressure* (psi)						Screen Factor	Viscosity (cp)
	$p_{6.4}$	$p_{12.7}$	$p_{28.6}$	$p_{50.8}$	$p_{95.3}$	$p_{139.7}$		
0	—	—	—	—	—	—	38.0	4.92
14.6	30	19.2	7.5	2.5	0.2	—	26.0	4.72
25.2	60	26.4	8.7	3.8	0.7	—	17.5	3.97
62.5	98	29.2	10.2	5.5	1.4	—	10.2	3.39
244	168	37.5	17	9.0	2.7	0.3	3.8	2.44
425	229	54	26	12.0	5.0	0.7	3.5	2.14
748	298	67	30	—	6.8	1.2	3.2	2.01

\*Pressure at radius  $r$ .

rates. The largest discrepancy occurs for pressure drops near the sandface. Two factors contribute to this discrepancy. First, the close proximity of the first pressure tap to the sandface introduces a relatively large experimental error simply because of the size of the hole used for the tap. Second, the model predicts a step-jump in the pressure profile at the sandface because of the nature of the entrance pressure drop.

Figs. 14 and 15 show the breakdown of the pressure contributions for the radial coreflood predictions (for the case where  $r$  is the external core radius) as a function of  $u_{max}/d_{gr}^2$ . As expected, the contributions associated with mechanical degradation and viscoelastic effects are greatest at the higher injection rates. Generally,  $\Delta p_{md}$  and  $A_p$  will dominate  $A_p$  when a small external radius is encountered. In field situations where the effective external radius is quite large,  $A_p$  should be more important. The importance of viscoelasticity relative to mechanical degradation is determined largely by the inner radius,  $r_w$ . Generally, the larger the inner radius, the more likely will  $A_p$  dominate  $\Delta p_{md}$ . Fig. 16 shows predicted and observed injectivities for the radial corefloods as a function of  $u_{max}/d_{gr}^2$ . For low values of  $u_{max}/d_{gr}^2$ , polymer solution injectivity is independent of injection rate. Polymer solution injectivity increases at higher injection rates because severe polymer mechanical degradation occurs.

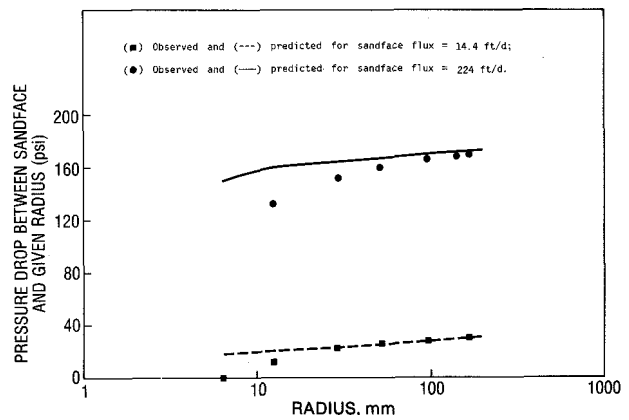


**Fig. 13—Radial coreflood results (600 ppm Polymer 6 in 3.3% brine; data from Table 8).**

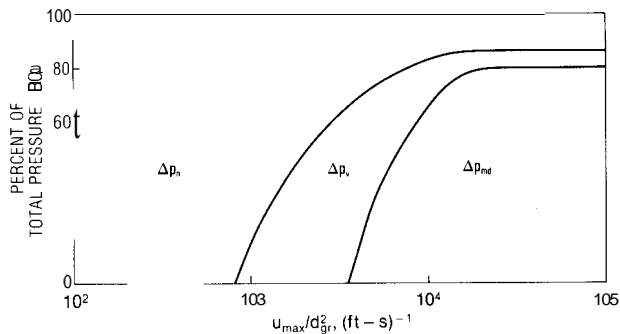


Fig. 14—Pressure contributions for radial core predictions (600 ppm Polymer A in 3.3% brine).

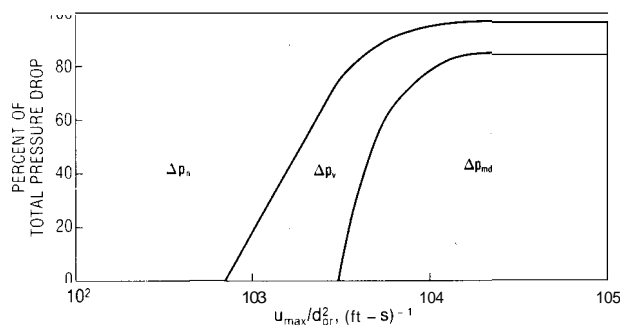


Fig. 15—Pressure contributions for radial core flood predictions (600 ppm Polymer B in 3.3% brine).

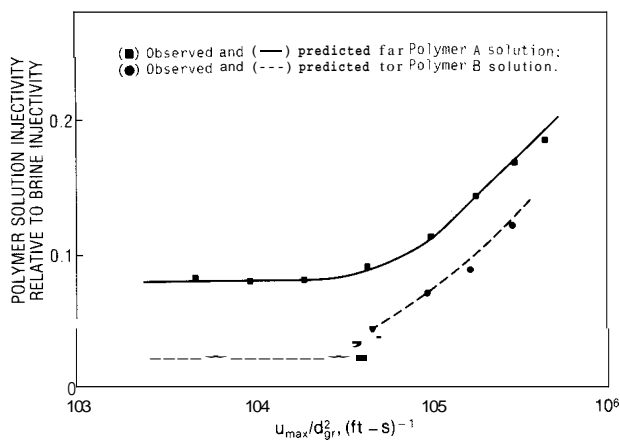


Fig. 16—Injectivity for radial corefloods.

## Application of the Injectivity Model to Injection Wells

When a polymer flood is initiated, significant injectivity losses are often observed. As mentioned earlier, several factors can be responsible for these losses. The model developed here can be used to estimate the degree of injectivity impairment caused by the rheological behavior of polyacrylamide solutions. This will aid in the diagnosis and correction of injectivity losses resulting from factors such as polymer flocculation of suspended particulate matter or inadequate polymer dispersal before injection.

The injection pressure drop [bottomhole pressure (BHP) minus average reservoir pressure],  $\Delta p$ , in Eq. 3 is given by

$$\Delta p = \Delta p_{md} + \Delta p_v + \Delta p_n + \Delta p_{ob} \quad \dots \dots \dots (12)$$

$\Delta p_{md}$  can be evaluated by using the  $u_{max}/d_{gr}^2$  correlation. If the injection rate is constant and the flow geometry is radial near a wellbore,  $\Delta p_r$  and  $\Delta p_i$  can be evaluated by using Eqs. 13 and 14:

$$\Delta p_n = \frac{q}{\theta h \lambda_b} (F_r)_{min} \ln \left( \frac{r_p}{r_w} \right), \quad \dots \dots \dots (13)$$

and

$$\Delta p_v = \frac{q}{\theta h \lambda_b} [(F_r)_{max} - (F_r)_{min}] \left[ 1 - \left( \frac{r_w}{r_p} \right)^n \right], \quad \dots \dots \dots (14)$$

where  $r_p$  is the radius associated with the polymer front. The development of Eqs. 13 and 14 is similar to that of Eqs. 10 and 11.  $\Delta p_{ob}$  is given by

$$\Delta p_{ob} = \frac{q}{I_b} - \frac{q}{\theta h \lambda_b} \ln \left( \frac{r_p}{r_w} \right), \quad \dots \dots \dots (15)$$

where  $I_b$  is the brine injectivity before polymer injection is started. Eqs. 13, 14, and 15 are valid when the polymer is flowing radially away from the wellbore. This is most likely to be true near the start of polymer injection, when the polymer front is not far from the wellbore.

## Conclusions

The following conclusions are relevant to the behavior of polyacrylamide solutions that contain 3% NaCl and 0.3% CaCl<sub>2</sub>. It is acknowledged that modification of some of these conclusions may be necessary when dealing with low-salinity polyacrylamide solutions.

1. Use of the  $u_{max}/d_{gr}^2$  correlation simplifies the prediction of mechanical degradation of polyacrylamide solutions. This correlation eliminates the need for an iterative procedure and is readily applied to any flow geometry.

2. If a polyacrylamide solution is degraded mechanically when injected into a porous medium, it will exhibit an "entrance pressure drop" upon crossing the sandface. The entrance pressure drop correlates well with  $u_{\max}/d_{gr}^2$ . Polyacrylamide mechanical degradation occurs very close to the inlet sandface.

3. For a polymer solution at a fixed level of mechanical degradation (constant screen factor), the resistance factor increases with increased flux.

4. A model that can be used to estimate injectivities of polyacrylamide solutions has been developed.

## Acknowledgments

I am grateful to H.S. Chi, J.M. Maerker, J.C. Roffall, and E.I. Sandvik for helpful discussions and for providing experimental data.

## Nomenclature

$d_{gr}$  = average grain diameter =

$$\frac{1-\phi}{\phi} \sqrt{\frac{150}{\phi}} k_b 1.0623 \times 10^{-14}, \text{ ft (m)}$$

$F_r$  = resistance factor

$(F_r)_{\max}$  = maximum resistance factor

$(F_r)_{\min}$  = minimum resistance factor

$F_s$  = screen factor

$h$  = height, ft (m)

$I_b$  = brine injectivity, B/D-psi ( $\text{m}^3/\text{d} \cdot \text{kPa}$ )

$I_p$  = polymer solution injectivity, B/D-psi ( $\text{m}^3/\text{d} \cdot \text{kPa}$ )

$k_b$  = effective brine permeability, md

$L_D$  = dimensionless length =  
(actual core length)/ $d_{gr}$

$m$  = empirical porosity exponent in Maerker correlation

$M$  = polymer molecular weight

$n$  = exponent in Eq. 4

$A_p$  = injection pressure drop (BHP minus average reservoir pressure), psi (kPa)

$\Delta p_{md}$  = entrance pressure drop associated with polymer mechanical degradation at the sandface, psi (kPa)

$\Delta p_n$  = pressure drop associated with polymer solutions flowing at low fluxes and exhibiting a Newtonian or flux-independent behavior, psi (kPa)

$\Delta p_{ob}$  = pressure drop associated with the flow of brine and oil, psi (kPa)

$\Delta p_v$  = pressure drop associated with dilatant or viscoelastic polymer behavior near a wellbore, psi (kPa)

$q$  = injection rate, B/D ( $\text{m}^3/\text{s}$ )

$r$  = radius, ft (m)

$r_p$  = radius of polymer front, ft (m)

$r_w$  = radius of wellbore, ft (m)

$u$  = flux, cu ft/sq ft/D ( $\text{m}^3/\text{m}^2/\text{s}$ )

$u_{\max}$  = maximum flux, cu ft/sq ft/D ( $\text{m}^3/\text{m}^2/\text{s}$ )

$\dot{\epsilon}$  = stretch rate =  $2(\text{flux})/(86,400 d_{gr} \phi)$ ,  
seconds $^{-1}$

$\theta$  = sector angle, degree (rad)

$\lambda_b$  = brine mobility, md/cp

$\lambda_p$  = polymer solution mobility, md/cp

$\mu$  = solution viscosity, cp ( $\text{Pa} \cdot \text{s}$ )

$\mu_s$  = solvent viscosity, cp (Pass)

$\phi$  = porosity, fraction

## Special Operator

ln = natural logarithm, base  $e$

## References

1. Pye, D.J.: "Improved Secondary Recovery by Control of Water Mobility," *J. Per. Tech.* (Aug. 1964) 911-16.
2. Smith, F.W.: "The Behavior of Partially Hydrolyzed Polyacrylamide Solutions in Porous Media," *J. Per. Tech.* (Feb. 1970) 148-56.
3. Maerker, J.M.: "Shear Degradation of Partially Hydrolyzed Polyacrylamide Solutions," *Soc. Pet. Eng. J.* (Aug. 1975) 311-22; *Trans.*, AIME, **259**.
4. Jennings, R.R., Rogers, J.H., and West, T.J.: "Factors Influencing Mobility Control by Polymer Solutions," *J. Per. Tech.* (March 1971) 391-401.
5. White, J.L., Goddard, J.E., and Phillips, H.M.: "Use of Polymers to Control Water Production in Oil Wells," *J. Per. Tech.* (Feb. 1973) 143-50.
6. Maerker, J.M.: "Mechanical Degradation of Partially Hydrolyzed Polyacrylamide Solutions in Unconsolidated Porous Media," *Soc. Pet. Eng. J.* (Aug. 1976) 172-74.
7. Morris, C.W. and Jackson, K.M.: "Mechanical Degradation of Polyacrylamide Solutions in Porous Media," paper SPE **7064** presented at the 1978 SPE Symposium on Improved Methods for Oil Recovery, Tulsa, April 16-19.
8. Gupta, S.P. and Trushenski, S.P.: "The Propagation of the Polymer Mobility Buffer Bank," *Soc. Pet. Eng. J.* (Feb. 1978) 5-11.
9. Mungan, N.: "Rheological Model for Ionic Polyacrylamide Solutions Over Extremely Wide Shear Rates," paper SPE 3521 presented at the 1971 SPE Annual Meeting, New Orleans, Oct. 3-6.
10. Gogarty, W.B.: "Mobility Control With Polymer Solutions," *Soc. Per. Eng. J.* (June 1967) 161-73.

## SI Metric Conversion Factors

cp	x 1.0*	E-03	= Pa · s
ft	x 3.048*	E-01	= m
in.	x 2.54*	E+00	= cm
psi	x 6.894 757	E+00	= kPa

\*Conversion factor is exact.

**SPEJ**

Original manuscript received in Society of Petroleum Engineers office July 19, 1980. Paper accepted for publication Dec. 6, 1982. Revised manuscript received Feb. 7, 1983. Paper (SPE 9297) first presented at the 1980 SPE Annual Technical Conference and Exhibition held in Dallas, Sept. 21-24.